

Partial Order Pruning: for Best Speed/Accuracy Trade-off in Neural Architecture Search

Xin Li¹ Yiming Zhou^{1,2} Zheng Pan¹ Jiashi Feng³

¹ UISEE.AI

² National Key Lab. of Communications, University of Electronic Science and Technology of China

³ Department of ECE, National University of Singapore

{xin.li, yiming.zhou, zheng.pan}@uisee.com elefjia@nus.edu.cn

Abstract

Achieving good speed and accuracy trade-off on target platform is very important in deploying deep neural networks. Most existing automatic architecture search approaches only pursue high performance but ignores such an important factor. In this work, we propose an algorithm “Partial Order Pruning” to prune architecture search space with partial order assumption, quickly lift the boundary of speed/accuracy trade-off on target platform, and automatically search the architecture with the best speed and accuracy trade-off. Our algorithm explicitly take profile information about the inference speed on target platform into consideration. With the proposed algorithm, we present several “Dongfeng” networks that provide high accuracy and fast inference speed on various application GPU platforms. By further searching decoder architecture, our DF-Seg real-time segmentation models yields state-of-the-art speed/accuracy trade-off on both embedded device and high-end GPU¹.

1. Introduction

Recent progress in computer vision is mostly driven by the advance of deep learning. Deploying deep convolutional neural networks (CNNs) on embedded devices becomes a hot research topic and is crucial in many application fields, such as self-driving where captured images need to pass through CNNs runnable on embedded devices for obtaining detailed semantic information. Different from high-end GPUs, the computation power of embedded devices is much more limited. This brings a lot of restrictions in deploying popular CNN models [10, 3]. Among them, one of the most serious problems is the inference speed will be slow for large-size CNN models. Although various approaches [28, 23] have been proposed to accel-

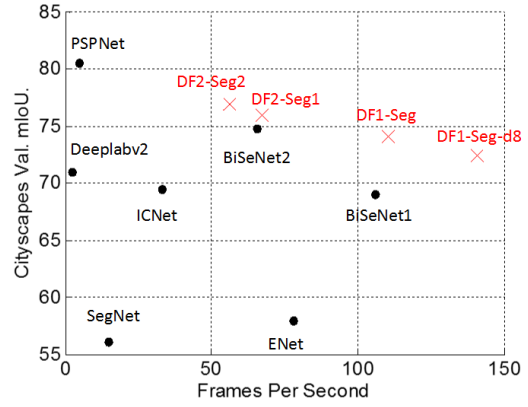


Figure 1. Speed (frames per second) and segmentation accuracy (mIoU_{class}) comparison on the Cityscapes [5] validation set. The compared models include PSPNet [29], Deeplabv2 [3], ENet [17], SegNet [1], ICNet [28], BiSeNet [26] and our DF-Seg models.

erate inference (e.g. pruning [9], quantization [23], factorization [14]), low-latency inference of CNN still remains unsolved. Reducing model size is a common practice at the cost of degraded performance. Furthermore, it is still an open question that what is the speed and accuracy trade-off “boundary” we can achieve on the target platform (e.g. TX2, GTX 1080Ti). In other words: given the maximum acceptable latency², what is the best accuracy one can get? To meet a certain accuracy requirements, what is the lowest latency one can expect? We aim to provide answers to these questions in this work.

Recently, various works have explored manually designed efficient model architectures [28, 26, 11, 20]. Most of these works adopt indirect metric, i.e. FLOPs, to estimate the computational complexity. However, it is observed that there is discrepancy between FLOPs and actual inference speed [15, 7]. Moreover, due to the characteristic differences of different hardware and software, it is hard to

¹Models have been release in <https://github.com/lixincn2015/Partial-Order-Pruning>.

²Latency is defined as inference time with batch size 1 in a CNN.

find a single architecture to be optimal for all the platforms. For example, some operations (*e.g.* 3×3 convolution in Nvidia GPUs [13]) are highly optimized by hardware and software design. The memory access that affects inference speed also differs on different platforms, and does not appear in the metric of FLOPs. Another line of works aim at automatically searching for the optimal network architecture. However, current network architecture searching algorithms [31, 18] mainly focus on exploring network architecture within individual block. More importantly, few algorithms [7, 24] directly consider actual inference speed into network architecture search.

In this paper, we focus on developing efficient architecture search algorithm to automatically select those networks offering better speed/accuracy trade-off on the target platform. Different from existing searching approaches, our proposed approach “Partial Order Pruning” (POP) utilizes actual latency to prune the search space with partial order assumption, and delves into lifting the boundary of speed/accuracy trade-off. The motivation behind our algorithm is intuitive. Along with the search procedure, some candidate architectures can be filtered out very early as they cannot provide better speed/accuracy trade-off given the partial order information. For example, a wider network cannot be more efficient than a narrower one with the same depth. By pruning search space based on this, our approach is able to focus on those architectures that are more likely to lift the boundary of speed/accuracy trade-off. *i.e.* searching for architectures provides higher accuracy at every latency. With proposed algorithm, we are able to obtain a set of “Dongfeng” (DF) networks that provide better accuracy and faster inference speed.

Our algorithm could also be applied to searching the architecture for specific components in semantic segmentation networks. The resulting DF-Seg models provide a new state-of-the-art in real-time urban scene parsing. Figure 1 provides a comparison between our segmentation networks and other methods. In sum, we make following contributions to network architecture search:

- We are among the first to delve into balancing the speed and accuracy of network architecture for network architecture search. By pruning search space with a partial order assumption, our “Partial Order Pruning” algorithm is able to efficiently lift the boundary of speed/accuracy trade-off.
- We present several “Dongfeng” networks that provide high accuracy and fast inference speed on embedded device, *i.e.* TX2. The accuracy of our DF1/DF2A networks are higher than ResNet18/50 on ImageNet validation set, but the inference latency is 43% and 39% lower, respectively.
- We apply the proposed algorithm to search decoder architecture for a segmentation network. Together with

DF backbone networks, we now achieve new state-of-the-art performance in real-time segmentation on both high-end GPU and embedded device. On GTX 1080Ti, our DF1-Seg model achieves 106.1 FPS at resolution 1024×2048 with $mIoU_{class}$ 74.1%. On TX2, our DF1-Seg model achieves 21.8 FPS at resolution 1280×720 , *i.e.* 720p.

2. Related Work

Efficient Network Designs In real application, light-weight CNN architectures [15, 11, 20] are more preferred to obtain a decent accuracy under limited computational budget. Group convolution plays a key role in these architectures. MobileNet_V2 [20] proposed an inverted residual module that uses group convolutions to reduce the memory footprint during inference. ShuffleNet [27] introduced pointwise group convolution and channel shuffle operation to reduce computation cost while maintaining accuracy. ShuffleNet_V2 [15] pointed out that there is a discrepancy between indirect metrics (FLOPs) and direct metrics (inference speed), and proposed four guidelines for efficient network design. However, these work design a single architecture without considering the underlying platform, and neither make efforts to lift the boundary of speed/accuracy trade-off on target platform. Our algorithm should be seen as complimentary to aforementioned works. We do not focus on manually designing sophisticated block, but make an effort to balance between depth and width in a network.

Model Architecture Search Various algorithms have been proposed to select network architecture automatically with either reinforcement learning [31, 30] or evolutionary algorithm [18, 19]. However, these algorithms still require significant computational resources, and the obtained networks are relatively slower than manually designed network [15, 7], even with comparable FLOPs. More recently, DPP-Net [7] takes platform-related objectives into consideration in architecture search, and searches for pareto-optimal network architectures. Even their goal is similar to ours to some extent, the search space and search algorithm of our work is totally different. Besides, aforementioned methods search the architecture in each individual. In contrast, we delve into balancing the width and depth of a network instead of designing sophisticated building block. Therefore, our work should be seen as complimentary to aforementioned works.

Real-time Semantic Segmentation Various models [29, 2, 4] have been proposed to pursue high performance, but their inference speed is relatively slow. In terms of fast semantic segmentation, early works [17, 1] employ relatively shallower backbone networks and lower image resolutions, offering fast inference speed but poorer accuracy. More recently, ICNet [28] proposed to use image cascade to speed

up the inference. Pre-trained deep CNN are only applied to the images with lowest resolution. BiSeNet [26] regards the common segmentation network as a context path, and employs an additional spatial path to preserve spatial information. However, none current real-time semantic segmentations have tried to accelerate inference by improving backbone network. Neither have they take characteristics of target platform into consideration. In contrast, our algorithm pursues better speed/accuracy trade-off in both backbone network and decoder network.

Model Acceleration Another line of researches aim at accelerating inference of a pre-trained network. This includes quantization [23], pruning [9], factorization [14]. More recently, NetAdapt [24] proposes to automatically adapt a pre-trained CNN to a mobile platform given a resource budget. Our approach is complimentary to these works.

3. Partial Order Pruning

3.1. Architecture Encoding

Figure 2(a) illustrates the general network architecture in our search space. The network compose of 6 stages to produce a classification result from input images. Stages 1~5 down-sample the spatial resolution of input tensor with a stride of 2, and stage 6 produces final prediction with a global average pooling and a fully connected layer. Stages 1&2 extract common low-level features on large tensor size, and bring heavy computation burden. In pursuit of efficient network, we only use one convolution layer in stage 1&2, *i.e.* *Conv1* and *Conv2*. We empirically find this is enough to achieve good accuracy. Each of stages 3, 4, 5 consists of L, M, N residual blocks respectively, where L, M, N are integers, *i.e.* $L, M, N \in \mathbb{N}$. Different settings of L/M/N lead to different network depth. Note that block number in each stage is mutually independent on others. The width (*i.e.* number of channels) of the i -th residual block in stage s is denoted as C_i^s . Therefore, an architecture can be encoded as shown in Figure 2(a). In practice, we restrict that $C_i^s \in \{64, 128, 256, 512, 1024\}$. We empirically restrict the width of a block to be not narrower than its preceding blocks. Throughout this paper, we use the basic residual block proposed in [10] if not mentioned otherwise. As shown in Figure 2(b), the building block consists of two convolution layers and a shortcut connection. Additional projection layer is added if the size of input does not match the output tensor. All convolutional layers are followed with a batch normalization [12] layer and ReLU nonlinearity.

3.2. Search Space Construction

All possible architectures, with different depth (number of blocks) and width (number of channel in each block), form the architecture search space, denoted as \mathbb{S} . The latency of architectures in \mathbb{S} can vary from very small number

to positive infinity. But we only care about architectures in a subspace $\hat{\mathbb{S}} \subset \mathbb{S}$ in practice, which provide latency in the range $[T_{min}, T_{max}]$.

We employ profiler provided by TensorRT library to obtain layer-wise latency of a network. We empirically found that a block with certain configuration (*i.e.* input/output tensor size) always consumes the same latency. Thus we can construct a look-up table $Latency(c_i, h_i, w_i, c_o, h_o, w_o)$ providing latency of each block configuration, where c_i/c_o are number of channels in input/output tensor, and $h_i/w_i/h_o/w_o$ are corresponding spatial size. For example, $Latency(32, 112, 112, 64, 56, 56) = 0.143\text{ms}$ on TX2. By simply summing up latency of each block, we can efficiently estimate the latency $Lat(x)$ of an architecture $x \in \mathbb{S}$. In Figure 3(a), we compare estimated latency with the profiled latency. It shows that our latency estimation highly close to the actual profiled latency. All architectures whose latency in range $[T_{min}, T_{max}]$ form up the subspace $\hat{\mathbb{S}}$. This subspace construction significantly narrow down our search space, and hence accelerate the architecture selection.

3.3. Partial Order Assumption

We find that there is a partial order relations among architectures, as illustrated in Figure 4. Let $x, y \in \hat{\mathbb{S}}$ denote two architectures in search space $\hat{\mathbb{S}}$, and $x \prec y$ denotes that x is shallower and narrower than y . In the following, we also call x a *precedent* of y if $x \prec y$. The pair (x, y) is called *comparable* if $x \prec y$ or $y \prec x$. Let $Acc(x)$ and $Lat(x)$ denote the accuracy and latency of architecture x . Then the partial order assumption of architectures can be summarized as follows: $\forall x, y \in \mathbb{S}, x \prec y$

$$Lat(x) \leq Lat(y), Acc(x) \leq Acc(y), \quad (1)$$

The above line assumes that the latency and accuracy of an architecture is both higher than its precedents. Note that this assumption may not be true for very deep networks that contains hundreds of layers [10]. But this assumption is generally true among the efficient architectures we care, *i.e.* $\hat{\mathbb{S}}$. We find all comparable architecture pairs $(x, y), x \prec y$ in our trained models (Section 4.2), and collect the latency difference $\Delta Lat = Lat(y) - Lat(x)$ and accuracy difference $\Delta Acc = Acc(y) - Acc(x)$ in each pair. As shown in Figure 3(b), most points locate in the first quartile. This means that accuracy of the precedent x is lower, in all most all comparable pairs. We also notice that a few points locate in the second quartile. But the lower limit of ΔAcc is -0.1% , which is negligible considering randomness in training process. The experimental result above verifies the reasonableness of our partial order assumption. The partial order assumption can be utilized to prune architecture search space, and speed up the search process significantly.

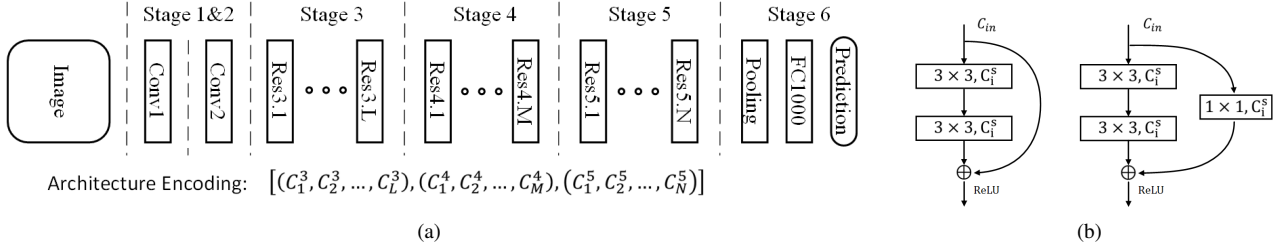


Figure 2. (a) Architecture encoding and (b) The residual block used throughout this paper.

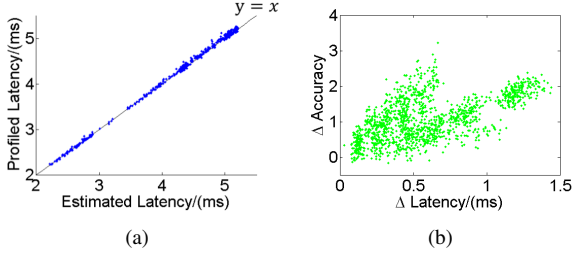


Figure 3. (a) Network latency estimation. (b) Validation of partial order assumption.

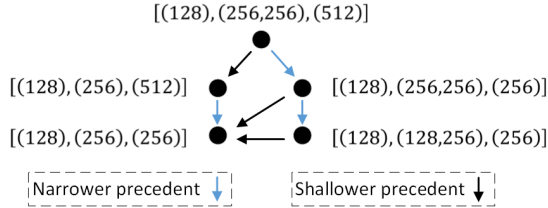


Figure 4. Partial order relations among architectures.

3.4. Partial Order Pruning

Formally, the goal of our architecture searching algorithm is to obtain a model with highest accuracy within every small latency range, i.e. $[T, T + \delta t]$:

$$\max_{x \in \hat{\mathcal{S}}} \text{Acc}(x), \text{ s.t. } \text{Lat}(x) \in [T, T + \delta t] \quad (2)$$

where δt is a short time (e.g. 0.1ms). Instead of searching individually at every small latency range, we optimize within entire latency range $[T_{min}, T_{max}]$. Benefit from our “Partial Order Pruning” (POP) algorithm, architecture searching at higher latency helps reduce the searching space at lower latency, and hence speed up the overall searching process.

We use a cutting plane algorithm to optimize the combinational optimization problem in Eqn. (2). Algorithm 1 summarize the pipeline of our POP algorithm. D is a set containing all trained architectures, and is initialized to be empty. P denotes the search space pruned from $\hat{\mathcal{S}}$. Everytime we train a new architecture $x \in \hat{\mathcal{S}} \setminus P$ and obtain its accuracy $\text{Acc}(x)$, we are able to update pruned search space P . Figure 5 illustrates how to construct P with the aforementioned partial order assumption. For each trained architecture $w \in D$, we find the fastest architecture $y_w \in D$

Algorithm 1 Partial Order Pruning

Initialize trained architecture set $D = \emptyset$
Initialize pruned architecture set $P = \emptyset$.
repeat
Random select an architecture $x \in \hat{\mathcal{S}} \setminus P$.
Train x and obtain its $\text{Acc}(x)$.
 $D \leftarrow D \cup \{x\}$.
for all $w \in D$ **do**
 $y_w = \arg \min_{y \in D} \text{Lat}(y), \text{ s.t. } \text{Acc}(y) \geq \text{Acc}(w)$
 $\Delta P_w = \{m \in \hat{\mathcal{S}} | m \prec w, \text{Lat}(m) \geq \text{Lat}(y_w)\}$
 $P \leftarrow P \cup (\bigcup_w \Delta P_w)$
end for
 $B(D) = \{x \in D | \forall m \in D, \text{Lat}(m) \geq \text{Lat}(x) \text{ or } \text{Acc}(m) \leq \text{Acc}(x)\}$
until No change to $B(D)$ for several iterations.

that provides better accuracy:

$$y_w \leftarrow \arg \min_{y \in D} \text{Lat}(y), \text{ s.t. } \text{Acc}(y) \geq \text{Acc}(w) \quad (3)$$

If no y_w is found that satisfies the condition, we continue to process the next w . Let ΔP_w denotes precedents of w with latency higher than y_w , i.e.

$$\Delta P_w = \{m \in \hat{\mathcal{S}} | m \prec w, \text{Lat}(m) \geq \text{Lat}(y_w)\} \quad (4)$$

Base on the partial order assumption, a precedent m has a lower latency and accuracy, i.e. $\text{Acc}(m) \leq \text{Acc}(w)$. Therefore, even though we do not actually train m , we can assume that:

$$\forall m \in \Delta P_w, \text{Acc}(m) \leq \text{Acc}(y_w) \quad (5)$$

In Figure 5, $\forall m \in \Delta P(w_i), i \in \{1, 2, 3\}$, the $(\text{Lat}(m), \text{Acc}(m))$ shall locate in corresponding shadow area. These architectures in ΔP_w are very unlikely to provide better speed/accuracy trade-off, and thus pruned from the search space to avoid unnecessary training cost.

Given trained architectures D , $B(D)$ denotes the architectures that provide best speed/accuracy trade-offs in trained models:

$$B(D) = \{x \in D | \forall w \in D, \text{Lat}(w) \geq \text{Lat}(x) \text{ or } \text{Acc}(w) \leq \text{Acc}(x)\} \quad (6)$$

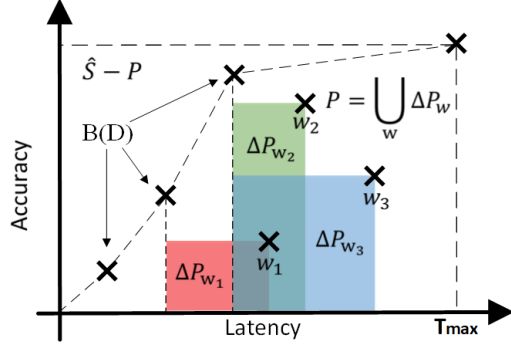


Figure 5. Partial order pruning. (Best viewed in color.)

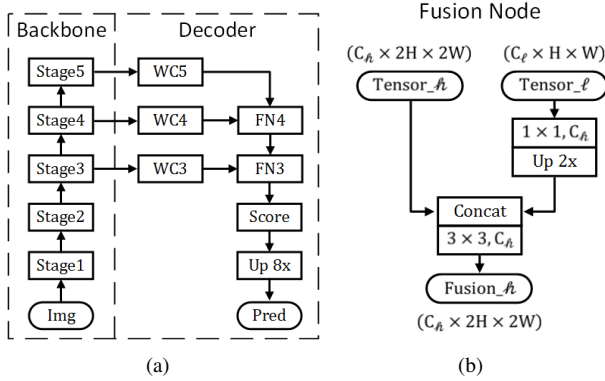


Figure 6. (a) Overall architecture of segmentation network. (b) Detailed architecture of the fusion node.

Models in $B(D)$ form the boundary for speed/accuracy trade-off we can achieve on target platform. Figure 5 illustrates $B(D)$ and corresponding speed/accuracy trade-off boundary. Intuitively, no architecture in $D \setminus B(D)$ could obtain higher accuracy with lower latency. By pruning P from search space \hat{S} , our POP algorithm speeds up the architecture search process, and delve into lifting the boundary of speed/accuracy trade-off. We stop the search process if no change to the $B(D)$ for several iterations.

3.5. Decoder Design

With the proposed POP algorithm 1, we are able to find backbone architectures that provide best speed/accuracy trade-offs on target platform. Given a backbone network, we build semantic segmentation networks as shown in Figure 6(a). Each stage in the backbone network down samples resolution by 2. The resolution of tensors in stage 5 is thus $1/32$ of the input image. These tensors are then processed by the decoder to produce final prediction.

We append a 1×1 convolution layer after stage 3/4/5 as “Width Controller” (WC). The width controllers reduce number of channels in corresponding stage without changing its spatial resolution. The decoder fuse tensors in different stages through the fusion nodes. The architecture of fusion node is shown in Figure 6(b). A fusion node first project low resolution tensor from C_ℓ channels to C_h chan-

nels with a 1×1 convolution layer, and then up-samples it by 2. We concatenate the up-sampled tensor with a higher resolution tensor, and then process it with a 3×3 convolution layer, to fuse the expressive power of different backbone stages. We fuse features from stage 3/4/5 and produce a $1/8$ resolution score map. The score map is then up-sampled by 8 and producing final per-pixel semantic segmentation prediction. We append a pyramid pooling module [29] after the output tensor of stage 5 to improve segmentation performance.

Let C^s , $s = 3, 4, 5$ denote the width of each WC. We heuristically set $C \in \{K, 32, 64, 128, 256, 512\}$, where K is number of classes. Given a backbone network, different settings of width controllers, i.e. $[C^3, C^4, C^5]$, lead to different decoder architectures. All the possible decoder WC settings form the search space of decoder architecture. Similar to backbone network architectures, we also assume there is a partial order relations among WC settings. That is, a narrower decoder is always more efficient and less accurate than a wider one. Therefore we can also employ POP algorithm to lift the speed/accuracy trade-off boundary in decoder architecture.

4. Experiments

4.1. Experimental Settings

Hardware and Software We adopt two typical kinds of hardwares that provide different computational power.

- Embedded device : We use Nvidia Jetson TX2 which is an embedded device with an integrated 256-core Pascal GPU. It provides considerable computational power with limited power consumption.
- High-end GPU : We use Nvidia Geforce GTX 1080Ti which is a high-end GPU that provides enormous computing power. We also use GTX Titan X (Maxwell) to provide a fair comparison with previous paper.

We adopt two kinds of inference speed measurement. First, we employ high-performance CNN inference framework TensorRT-3.0.4, and report corresponding inference speed. This ensures that our results and observations have significance in practice. Second, for a fair comparison with ICNet [28], we use the time measure tool “Caffe time”, and obtain average inference time by setting the repeating number to 100. All experiments are performed under CUDA 9.0 and CUDNN V7.

Benchmark Datasets We conduct experiments on two benchmark datasets. The ILSVRC 2012, *a.k.a* ImageNet [6] is a large scale image classification benchmark dataset. There are over 1.2 million color images in the training set, and 50k color images in the validation set. The Cityscapes is a large scale benchmark dataset for urban scene parsing. The 5,000 images with high quality

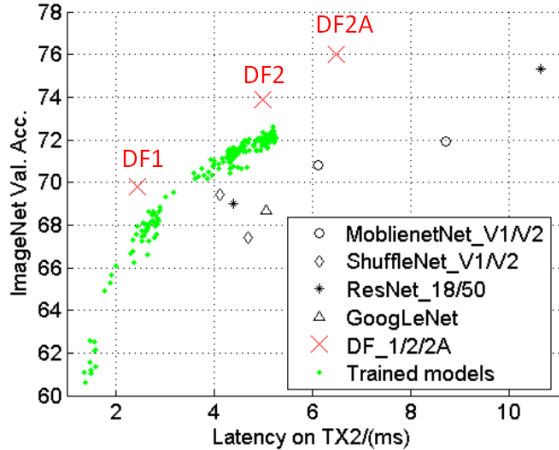


Figure 7. Backbone network searching results.

Model	Top1 Acc.	Latency (ms)	FLOPs
ShuffleNet_V2 [15]	69.4%	4.1	146M
ResNet-18 [10]	69.0%	4.4	1.8G
ShuffleNet_V1 [27]	67.4%	4.7	140M
GoogLeNet [21]	68.7%	5.1	1.43G
MobileNet_V1 [11]	70.8%	6.1	569M
MobileNet_V2 [20]	71.9%	8.7	300M
ResNet-50 [10]	75.3%	10.6	3.8G
DF1	69.8%	2.5	746M
DF2	73.9%	5.0	1.77G
DF2A	76.0%	6.5	1.97G

Table 1. Comparison with popular backbone models on TX2.

pixel-level annotations are split to 2,975 for training, 500 for validation, and 1,525 for testing.

4.2. Backbone Architecture Search

In contrast to current architecture search algorithms that train on small dataset, we directly conduct architecture searching on ImageNet. We use the SGD optimizer with poly learning rate policy to train models. The power is set to 2, and the momentum is set to 0.9. We use a standard weight decay of 0.0001. The batch size is set to 2048 to accelerate training process. As observed by previous works [25, 8], large batch size leads to overfitting. We employ data augmentation methods including random scaling and stretching to avoid the overfitting problem. Following guidelines in [8], we first train each model for 5 epochs with learning rate 0.1 as a warm up scheme, to overcome the optimization challenges early in training. Then we train each model for 80 epochs with a initial learning rate 0.8.

We conduct backbone architecture searching experiments on TX2 platform. During the search process, we evaluate the single crop Top-1 accuracy on ImageNet validation set and the inference latency at resolution 224×224 . We have a great interest in efficient architectures whose la-

tency are in the range $[1ms, 5ms]$, and construct the search space $\hat{\mathbb{S}}$ accordingly (Section 3.2). We conduct architecture search with Algorithm 1, and stopped the search process when no remarkable boundary update was found during the search. The resulting speed/accuracy trade-off boundary is considered to be near optimal in our search space $\hat{\mathbb{S}}$, on target platform TX2. We have trained ~ 200 models in total, as shown in Figure 7. While the training configuration is kept the same during architecture search, we also train two representative network architectures with additional supervision [21], to further improve their accuracy. The resulting models are referred to as DF1, DF2. We further replace some of the building block in DF2 from basic block in Figure 2(b) to bottleneck block [10], the resulting model is referred to as DF2A. Table 2 provides detailed architectures of our three DF models. Figure 7 and Table 1 provide a comparison between our backbone networks and popular models on the target platform TX2. Training with more sophisticated methods (*e.g.* dropout, label smoothing) may provide higher accuracy, but it is not the focus of this paper.

Comparing to ResNet-18 and GoogLeNet, our DF1 model obtains a higher accuracy (*i.e.* 69.8%) but the inference latency is 43% and 51% lower respectively, our DF2 model has a similar latency but the accuracy is 4.9% and 5.2% higher respectively. Further more, our DF2A model obtains a surpassing ResNet-50-level accuracy with a 39% lower latency. Note that we are using same building blocks with ResNet-18/50. So we attribute the better speed/accuracy trade-off to the better balancing between depth and width in our architectures. Specifically, our DF1/DF2A models are apparently slimmer and deeper than ResNet-18/50 to obtain the same accuracy.

MobileNet_V1/V2 and ShuffleNet_V1/V2³ are state-of-the-art efficient models that initially designed for mobile applications. We have also compare our DF models to them on TX2 in Table 1 and Figure 7. Comparing to MobileNet/ShuffleNet, our DF1 model achieve higher accuracy, but lower inference latency. The MobileNet/ShuffleNet has less FLOPs but higher latency. This is because MobileNet/ShuffleNet have higher memory access cost. The total memory cost (*i.e.* intermediate features) of ShuffleNet_V2 and DF1 are 4.86M and 2.91M respectively. This indicates that indirect metric (*i.e.* FLOPs) may be inconsistent with direct metric (*i.e.* latency) on target platform [22, 15]. Therefore, taking hardware and software characteristic into consideration is necessary to achieve the best speed/accuracy trade-off.

Search efficiency Figure 8(a) shows the number of pruned architectures in the search process. We have pruned 438 architectures after training 200 models, covering 638 architectures in search space $\hat{\mathbb{S}}$. Therefore, our POP algorithm accelerates the architecture search process for 2.2

³We report the latency with our re-implementation.

Stage	Layer	Output size	DF1	DF2	DF2A
1	Conv1	112×112	$3 \times 3, 32$	$3 \times 3, 32$	$3 \times 3, 32$
2	Conv2	56×56	$3 \times 3, 64$	$3 \times 3, 64$	$3 \times 3, 64$
3	Res3_x	28×28	$\begin{bmatrix} 3 \times 3, 64 \\ 3 \times 3, 64 \end{bmatrix} \times 3$	$\begin{bmatrix} 3 \times 3, 64 \\ 3 \times 3, 64 \end{bmatrix} \times 2$ $\begin{bmatrix} 3 \times 3, 128 \\ 3 \times 3, 128 \end{bmatrix} \times 1$	$\begin{bmatrix} 3 \times 3, 64 \\ 3 \times 3, 64 \end{bmatrix} \times 2$ $\begin{bmatrix} 3 \times 3, 128 \\ 3 \times 3, 128 \end{bmatrix} \times 1$
4	Res4_x	14×14	$\begin{bmatrix} 3 \times 3, 128 \\ 3 \times 3, 128 \end{bmatrix} \times 3$	$\begin{bmatrix} 3 \times 3, 128 \\ 3 \times 3, 128 \end{bmatrix} \times 10$ $\begin{bmatrix} 3 \times 3, 256 \\ 3 \times 3, 256 \end{bmatrix} \times 1$	$\begin{bmatrix} 1 \times 1, 128 \\ 3 \times 3, 128 \\ 1 \times 1, 512 \end{bmatrix} \times 10$ $\begin{bmatrix} 1 \times 1, 256 \\ 3 \times 3, 256 \\ 1 \times 1, 1024 \end{bmatrix} \times 1$
5	Res5_x	7×7	$\begin{bmatrix} 3 \times 3, 256 \\ 3 \times 3, 256 \end{bmatrix} \times 3$ $\begin{bmatrix} 3 \times 3, 512 \\ 3 \times 3, 512 \end{bmatrix} \times 1$	$\begin{bmatrix} 3 \times 3, 256 \\ 3 \times 3, 256 \end{bmatrix} \times 4$ $\begin{bmatrix} 3 \times 3, 512 \\ 3 \times 3, 512 \end{bmatrix} \times 2$	$\begin{bmatrix} 1 \times 1, 256 \\ 3 \times 3, 256 \\ 1 \times 1, 1024 \end{bmatrix} \times 4$ $\begin{bmatrix} 1 \times 1, 512 \\ 3 \times 3, 512 \\ 1 \times 1, 1024 \end{bmatrix} \times 2$
6	FC	1×1	Global Average Pooling, 1000-d FC, Softmax.		
Depth			23	43	60

Table 2. Architecture of DF models.

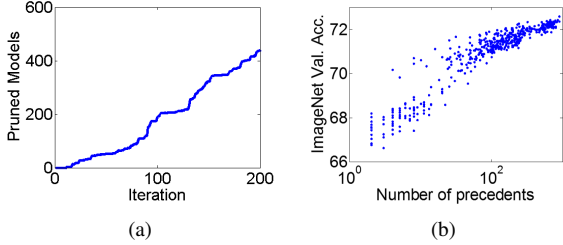


Figure 8. (a) Number of pruned models. (b) Accuracy is related to number of precedents.

times. Each model takes 5 ~ 7 hours on a server with 8-GPUs. Training the 200 models takes ~ 400 GPU days in total. The computational cost of our architecture searching on ImageNet is lower than building block searching [31, 18] on CIFAR-10 by an order.

Good practices Based on our architecture search results, we make following observations. 1) Very quick down-sampling is preferred in early stages to obtain higher efficiency. We use 1 convolutional layer in each of stage 1&2, and are still able to achieve good accuracy. 2) Down-sampling with convolutional layer is preferred than pooling layer to obtain higher accuracy. We only use 1 global average pooling at the end of the network. 3) We empirically find that the accuracy of a network is correlated to the number of its precedents, as shown in Figure 8(b). We assume that an architecture with more precedents may have a better balance between depth and width.

4.3. Decoder Architecture Search

With our DF1/DF2 backbone network, we conduct decoder architecture search experiments on two platforms,

Method	mIoU _{class}		FPS	FPS (Caffe)
	val	test		
SegNet [1]	-	56.1	-	-
ENet [17]	-	58.3	-	-
ICNet [28]	67.7	69.5	-	30.3
ESPNet [16]	-	60.3	110	-
BiSeNet1 [†] [26]	69.0	68.4	105.8	-
BiSeNet2 [†] [26]	74.8	74.7	65.5	-
DF1-Seg	74.1	73.0	106.1	30.7
DF2-Seg1	75.9	74.8	67.2	20.5
DF2-Seg2	76.9	75.3	56.3	17.7
DF1-Seg-d8	72.4	71.4	136.9	40.2

Table 3. Comparison with other real-time segmentation models on 1080Ti. [†] represents that FPS is evaluated at 1536×768 .

1080Ti and TX2. The mIoU_{class} at resolution 1024×2048 is evaluated as a metric of segmentation accuracy. The profiler of TensorRT is employed to evaluate latency of segmentation networks. We evaluate latency at resolution 1024×2048 on 1080Ti, and 640×360 on TX2.

Figure 9 illustrates our decoder architecture search results. We select three segmentation networks (*i.e.* DF1-Seg, DF2-Seg1, DF2-Seg2) from trained networks that provide good speed/accuracy trade-off on both TX2 and 1080Ti, which are referred to as DF-Seg series models. The WC setting in the decoder of three segmentation networks are [19, 32, 128], [19, 19, 32], [19, 256, 512] respectively (19 corresponds the number of classes). Few previous works have report their inference speed on TX2, so we provide a comparison between our DF-Seg models and other methods on 1080Ti, as shown in Table 3. We note that IC-

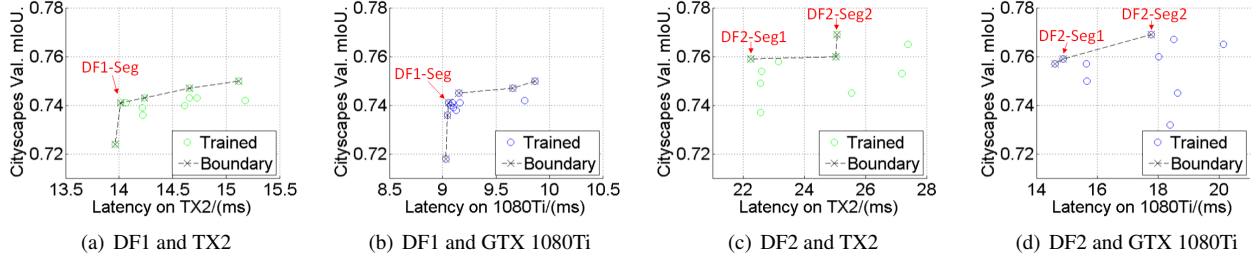


Figure 9. Speed/accuracy trade-off of decoder architecture search results with different backbone networks on different platforms. DF1-Seg/DF2-Seg are two segmentation networks provide good speed/accuracy trade-off on both TX2 and GTX 1080Ti.

Net [28] explicitly explained their inference speed measurement. Therefore, we add additional column “FPS(Caffe)” in Table 3 for a fair comparison. Inference speed in the “FPS(Caffe)” column are measured by “Caffe time”, on Titan X (Maxwell), at resolution 1024×2048 too.

Comparing to BiSeNet1, our DF1-Seg achieves comparable inference speed (106.1 FPS vs 105.8 FPS), but the $mIoU_{class}$ on test set is 4.6% higher (73.0% vs 68.4%). Comparing to BiSeNet2, our DF1-Seg achieves comparable $mIoU_{class}$ on validation set (74.1% vs 74.8%), but the inference speed (FPS) is 1.62 times faster (106.1 FPS vs 65.5 FPS). We attribute the better speed/accuracy trade-off of DF1-Seg to its backbone network DF1. BiSeNet2 employs ResNet-18 as backbone network. Our DF1 has a comparable accuracy with ResNet-18, but is 1.76 times faster (2.5ms vs 4.4ms), as shown in Table 1. Comparing to ICNet [28], DF1-Seg achieves comparable inference speed, and the $mIoU_{class}$ is 3.5% higher on test set (73.0% vs 69.5%). Our DF2-Seg1 model also achieve faster inference speed and better segmentation accuracy than BiSeNet2. With a wider decoder setting ([19, 256, 512]), our DF2-Seg2 model achieves the best $mIoU_{class}$ 76.9% on validation set and 75.3% on test set at 56.3 FPS.

We obtain an even faster segmentation network by dropping the final up-sampling layer, and produce a prediction at 1/8 of input resolution. The images to segment are then up-sampled by 8 times with nearest neighbor interpolation, which can be implemented very efficiently. By this way, we obtain a DF1-Seg-d8 network that achieves 136.9 FPS on 1080Ti, and is the $mIoU_{class}$ on test set (71.4%) is still 1.9% and 3% better than ICNet (69.5%) and BiSeNet1 (68.4%), respectively.

The experiments above show that the DF-Seg series segmentation networks achieve new state-of-the-art in real-time segmentation on high-end GPU, demonstrating they offer better speed/accuracy trade-offs.

Speed analyze on Titan X (Maxwell) For a fair comparison with previous methods, we compare inference speed in Table 4 on Titan X (Maxwell) at different resolution. Our DF1-Seg and DF1-Seg-d8 achieve 59.9 FPS and 75.9 FPS at resolution 1920×1080 , *i.e.* 1080p. This verifies that we

Method	640×360 ms / FPS	1280×720 ms / FPS	1920×1080 ms / FPS
SegNet [1]	69/14.6	289/3.5	637/1.6
ENet [17]	7/135.4	21/46.8	46/21.6
BiSeNet-1 [26]	5/203.5	12/82.3	24/41.4
BiSeNet-2 [26]	8/129.4	21/47.9	43/23
DF1-Seg	3.65/274.0	8.24/121.4	16.70/59.9
DF2-Seg1	5.88/170.1	13.43/74.5	27.36/36.5
DF2-Seg2	6.57/152.2	15.10/66.2	31.08/32.2
DF1-Seg-d8	3.25/307.7	6.62/151.1	13.18/75.9

Table 4. Speed analyze on Titan X (Maxwell).

Method	480×320 ms / FPS	640×360 ms / FPS	1280×720 ms / FPS
ESPNet [16]	-/-	-/~20	-/-
DF1-Seg	9.45/105.8	14.01/71.4	45.93/21.8
DF2-Seg1	15.32/65.3	22.25/44.9	73.32/13.6
DF2-Seg2	16.98/58.9	25.07/39.9	82.07/12.2
DF1-Seg-d8	7.48/133.7	10.79/92.7	33.41/29.9

Table 5. Speed analyze on TX2.

have achieved new state-of-the-art real-time segmentation on high-end GPU.

Speed analyze on TX2 Previous works [1, 17] mostly adopt TX1 as the embedded device to analyze their inference speed. In Table 5, we provide a detailed inference speed analyze on TX2. Our DF1-Seg and DF1-Seg-d8 achieved 21.8 FPS and 29.9 FPS at resolution 1280×720 , *i.e.* 720p.

5. Conclusion

We have proposed a network architecture search algorithm “Partial Order Pruning” (POP). It takes platform characteristics into consideration, and is devoted to lifting the boundary of speed/accuracy trade-off on target platform. By utilizing partial order assumption, it efficiently prunes feasible architecture space to speed up the search process. We employ the proposed algorithm in searching for both the backbone network and decoder network architec-

ture. The searched DF backbone models provide state-of-the-art speed/accuracy trade-off on target platform. The searched DF-Seg series real-time segmentation networks have achieved state-of-the-art speed/accuracy trade-off on both embedded device and high-end GPU.

References

- [1] V. Badrinarayanan, A. Kendall, and R. Cipolla. Segnet: A deep convolutional encoder-decoder architecture for image segmentation. *TPAMI*, (12):2481–2495, 2017. 1, 2, 7, 8
- [2] L.-C. Chen, M. D. Collins, Y. Zhu, G. Papandreou, B. Zoph, F. Schroff, H. Adam, and J. Shlens. Searching for efficient multi-scale architectures for dense image prediction. *NIPS*, 2018. 2
- [3] L.-C. Chen, G. Papandreou, I. Kokkinos, K. Murphy, and A. L. Yuille. Deeplab: Semantic image segmentation with deep convolutional nets, atrous convolution, and fully connected crfs. *TPAMI*, 40(4):834–848, 2018. 1
- [4] L.-C. Chen, Y. Zhu, G. Papandreou, F. Schroff, and H. Adam. Encoder-decoder with atrous separable convolution for semantic image segmentation. *ECCV*, 2018. 2
- [5] M. Cordts, M. Omran, S. Ramos, T. Rehfeld, M. Enzweiler, R. Benenson, U. Franke, S. Roth, and B. Schiele. The cityscapes dataset for semantic urban scene understanding. *CVPR*, 2016. 1
- [6] J. Deng, W. Dong, R. Socher, L.-J. Li, K. Li, and L. Fei-Fei. Imagenet: A large-scale hierarchical image database. In *CVPR*, 2009. 5
- [7] J.-D. Dong, A.-C. Cheng, D.-C. Juan, W. Wei, and M. Sun. Dpp-net: Device-aware progressive search for pareto-optimal neural architectures. *ECCV*, 2018. 1, 2
- [8] P. Goyal, P. Dollár, R. Girshick, P. Noordhuis, L. Wesolowski, A. Kyrola, A. Tulloch, Y. Jia, and K. He. Accurate, large minibatch sgd: training imagenet in 1 hour. *arXiv preprint arXiv:1706.02677*, 2017. 6
- [9] Y. Guo, A. Yao, and Y. Chen. Dynamic network surgery for efficient dnns. *NIPS*, 2016. 1, 3
- [10] K. He, X. Zhang, S. Ren, and J. Sun. Deep residual learning for image recognition. *CVPR*, 2016. 1, 3, 6
- [11] A. G. Howard, M. Zhu, B. Chen, D. Kalenichenko, W. Wang, T. Weyand, M. Andreetto, and H. Adam. Mobilenets: Efficient convolutional neural networks for mobile vision applications. *arXiv preprint arXiv:1704.04861*, 2017. 1, 2, 6
- [12] S. Ioffe and C. Szegedy. Batch normalization: Accelerating deep network training by reducing internal covariate shift. *ICML*, 2015. 3
- [13] A. Lavin and G. Scott. Fast algorithms for convolutional neural networks. *CVPR*, 2016. 2
- [14] B. Liu, M. Wang, H. Foroosh, M. Tappen, and M. Pensky. Sparse convolutional neural networks. *CVPR*, 2015. 1, 3
- [15] N. Ma, X. Zhang, H.-T. Zheng, and J. Sun. Shufflenet v2: Practical guidelines for efficient cnn architecture design. *ECCV*, 2018. 1, 2, 6
- [16] S. Mehta, M. Rastegari, A. Caspi, L. Shapiro, and H. Hajishirzi. Espnet: Efficient spatial pyramid of dilated convolutions for semantic segmentation. *ECCV*, 2018. 7, 8
- [17] A. Paszke, A. Chaurasia, S. Kim, and E. Culurciello. Enet: A deep neural network architecture for real-time semantic segmentation. *arXiv preprint arXiv:1606.02147*, 2016. 1, 2, 7, 8
- [18] E. Real, A. Aggarwal, Y. Huang, and Q. V. Le. Regularized evolution for image classifier architecture search. *arXiv preprint arXiv:1802.01548*, 2018. 2, 7
- [19] E. Real, S. Moore, A. Selle, S. Saxena, Y. L. Suematsu, J. Tan, Q. Le, and A. Kurakin. Large-scale evolution of image classifiers. *ICML*, 2017. 2
- [20] M. Sandler, A. Howard, M. Zhu, A. Zhmoginov, and L.-C. Chen. Inverted residuals and linear bottlenecks: Mobile networks for classification, detection and segmentation. *CVPR*, 2018. 1, 2, 6
- [21] C. Szegedy, W. Liu, Y. Jia, P. Sermanet, S. Reed, D. Anguelov, D. Erhan, V. Vanhoucke, and A. Rabinovich. Going deeper with convolutions. *CVPR*, 2015. 6
- [22] R. J. Wang, X. Li, S. Ao, and C. X. Ling. Pelee: A real-time object detection system on mobile devices. *NIPS*, 2018. 6
- [23] J. Wu, C. Leng, Y. Wang, Q. Hu, and J. Cheng. Quantized convolutional neural networks for mobile devices. *CVPR*, 2016. 1, 3
- [24] T.-J. Yang, A. Howard, B. Chen, X. Zhang, A. Go, M. Sandler, V. Sze, and H. Adam. Netadapt: Platform-aware neural network adaptation for mobile applications. *ECCV*, 2018. 2, 3
- [25] Y. You, I. Gitman, and B. Ginsburg. Scaling sgd batch size to 32k for imagenet training. *arXiv preprint arXiv:1708.03888*, 2017. 6
- [26] C. Yu, J. Wang, C. Peng, C. Gao, G. Yu, and N. Sang. Bisenet: Bilateral segmentation network for real-time semantic segmentation. *ECCV*, 2018. 1, 3, 7, 8
- [27] X. Zhang, X. Zhou, M. Lin, and J. Sun. Shufflenet: An extremely efficient convolutional neural network for mobile devices. *CVPR*, 2018. 2, 6
- [28] H. Zhao, X. Qi, X. Shen, J. Shi, and J. Jia. Icnnet for real-time semantic segmentation on high-resolution images. *ECCV*, 2018. 1, 2, 5, 7, 8
- [29] H. Zhao, J. Shi, X. Qi, X. Wang, and J. Jia. Pyramid scene parsing network. *CVPR*, 2017. 1, 2, 5
- [30] B. Zoph and Q. V. Le. Neural architecture search with reinforcement learning. *ICLR*, 2017. 2
- [31] B. Zoph, V. Vasudevan, J. Shlens, and Q. V. Le. Learning transferable architectures for scalable image recognition. *CVPR*, 2018. 2, 7